Journal of Orthopaedic Translation 21 (2020) 35–40

Contents lists available at ScienceDirect

Journal of Orthopaedic Translation

journal homepage: www.journals.elsevier.com/journal-of-orthopaedic-translation

Original Article

Population-based design and 3D finite element analysis of transforaminal thoracic interbody fusion cages

Yifeng Yu [a,☆], Wenjing Li [b,☆], Lingjia Yu [c], Hao Qu [a], Tong Niu [a], Yu Zhao [a,*]

[a] Department of Orthopaedics, Peking Union Medical College Hospital, Chinese Academy of Medical Sciences and Peking Union Medical College, Beijing, China
[b] Department of Orthopaedics, Beijing Jishuitan Hospital, Beijing, China
[c] Department of Orthopaedics, Beijing Friendship Hospital, Beijing, China

ARTICLE INFO

Keywords:
Anatomy parameters
Finite element analysis
Thoracic interbody cage

ABSTRACT

Objective: To compare the biomechanical characteristics of two transforaminal thoracic interbody fusion cages based on the Chinese population thoracic anatomy.
Method: Computed tomography scans of the thoracic spine of 150 patients from our institution were collected and analysed. Two cages were designed based on the anatomical parameters of these patients. Further, we used 3D finite element analysis models to compare the stability of two cages by using Mimics 17.0 and ANSYS 15.0 software.
Result: Two kinds of thoracic cages (box and kidney-shaped) were designed. Under the displacement working condition, the two new fusion cages could achieve immediate postoperative stability, but the kidney-shaped cage was better than the box-shaped cage. Under the stress working condition, no highly focused stress area was found in either cages, but the kidney-shaped cage experienced less stress than the box-shaped cage.
Conclusion: The kidney-shaped cage is more stable and experiences lesser stress than the box-shaped cage after thoracic intervertebral fusion, and it is more suitable for Chinese transforaminal thoracic interbody fusion.
The translational potential of this article: This article is about thoracic fusion cage design and finite element analysis (FEA) analysis based on the thoracic anatomy parameters. For there is currently no suitable thoracic fusion cage for transforaminal thoracic interbody fusion, the results in this article may have the potential of transferring the two designed cages into clinical use.

Introduction

Thoracic spinal stenosis (TSS) is a common cause of myelopathy in the East Asian population, which can cause serious adult disability and be a heavy burden to the family and society [1]. Machino et al. [2] in 2010 first proposed the concept of "transforaminal thoracic interbody fusion"(TTIF), inspired by the "transforaminal lumbar interbody fusion," for treating thoracic spinal diseases. This new operation has been succeessfully applied to 10 patients, and these 10 patients have achieved complete decompression and three-column fusion. Compared with other thoracic spinal approaches, TTIF is characterised by less damage and shorter recovery time. In addition, it results in immediate postoperative stability and maintenance of physiological curve in the thoracic spine, indicating a good outlook for its application [3,4]. This may be a new way to accomplish sufficient decompression with less surgical complications. However, TTIF is limited because of the lack of suitable thoracic intervertebral cages. Given that no specific fusion cage was available, surgeons only use intervertebral compression bone grafting for thoracic intervertebral fusion [4,5]. However, either autogenous bone or allogeneic bone grafting has its own disadvantages, which may cause complications to patients [6]. Compared with bone grafting, interbody cages could provide better mechanical strength [7] and postoperative fusion stability, as well as lesser stress in the pedicle screw fixation system, which may reduce postoperative screw fracture or broken rod rate [8,9]. At present, the available thoracic spine parameters were only investigated among the Europe or the United States population, and there is a lack of research on the thoracic anatomical

* Corresponding author. Department of Orthopaedics, Peking Union Medical College Hospital, Chinese Academy of Medical Sciences and Peking Union Medical College, Dong Cheng District Shuai Fu Yuan No.1, Beijing, 100730, China.
E-mail addresses: yuyi9707@163.com (Y. Yu), sunshine_lwj@163.com (W. Li), drjackyu@126.com (L. Yu), quhao7011@126.com (H. Qu), niutong9494@163.com (T. Niu), zhaoyupumch@126.com (Y. Zhao).
☆ Yifeng Yu and Wenjing Li contributed equally to this article.

https://doi.org/10.1016/j.jot.2019.12.006
Received 8 September 2019; Received in revised form 12 December 2019; Accepted 16 December 2019
Available online 9 January 2020

parameters of the Chinese population. The thoracic vertebral fusion cages should be designed based on the characteristic of the anatomical parameters of Chinese patients. With the rapid development of computer-aided technology, owing to its lower cost and repetition, the finite element analysis (FEA) has been widely used in spinal biomechanical tests [10–12]. In this study, the finite element models of thoracic spinal fusion with two different kinds of designed cages were established. The shift and stress parameters under different conditions (flexion, extension and rotation) were measured to compare the stability and stress distribution between the two newly designed thoracic interbody fusion cages for TTIF.

Materials and methods

Data collection

This research was accomplished in Peking Union Medical College Hospital , Beijing, China.

Computed tomography (CT) scans (SOMATOM Definition Flash, Siemens) of the thoracic spine of 150 patients from our institution were collected (inclusion criteria: age $\geq$ 18 years old, male or female, with informed consent; exclusion criteria: patients combined with spinal disease which may cause abnormal anatomical structure of thoracic interbody including spinal deformity, trauma, infection, tumour, fracture, inflammation, and combined with systemic metabolic diseases, congenital disease–induced spine dysplasia, severe degenerative spinal disease, and patients without informed consent). Patients were placed in a supine position when undergoing CT scans, which were saved in standard Digital Imaging and Communications in Medicine (DICOM) format. The thoracic interbody parameters of thoracic segment 10 to 12 (T10-12) are measured using Mimics 17.0 software, Materialise, Belgium (Fig. 1) because thoracic stenosis most commonly occur at these levels [13].

Parameter measurement

In the central sagittal plane (Fig. 1A), intervertebral height was measured in three positions (anterior, median and posterior). Anterior disc height was measured from the anterior of the vertebrae at levels T10 to T12. Median disc height was defined as the centre of vertebral levels T10 and T12. Posterior disc height was defined as the distance from the posterior of the vertebrae at levels T10 to T12. Moreover, foraminal height was the distance between the midpoint of the upper part of the inferior vertebral pedicle and the lower part of the upper vertebral pedicle. The results are shown in Table 1.

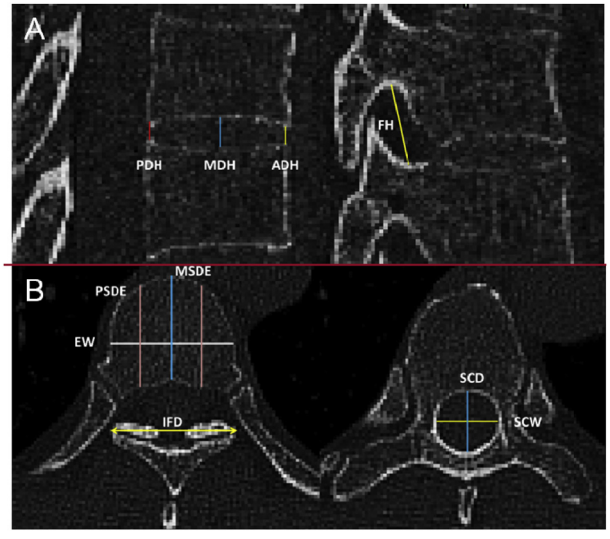

Figure 1. (A) Measurement of intervertebrae and foramen (B) Measurement of vertebrae and spinal canal.

Table 1
Measurement of anatomical parameters of the thoracic vertebrae in the sagittal position (mm).

	Height of intervertebral space			FH
	ADH	MDH	PDH	
T10/11	4.92 ± 0.93	7.33 ± 0.84	3.76 ± 0.72	14.36 ± 1.27
T11/12	5.59 ± 1.03	7.85 ± 1.05	4.18 ± 0.83	15.93 ± 1.34

ADH, anterior disc height; MDH, median disc height; PDH, posterior disc height; FH: foraminal height.

In the cross-sectional plane (Fig. 1B), endplate width (EW) was defined as the horizontal distance between the two sides of the bony endplate. Median sagittal diameter of endplate was the midpoint of the anterior border and the posterior of the bony endplate. The paramedian sagittal diameter of endplate divided the endplate into four parts, (vertical to transverse diameter through the 1/4 and 2/4 junctions or the axis of the 3/4 and 4/4 junctions). Spinal canal width was defined as the distance between the inner edges of the pedicle on both sides of the same segment. Spinal canal depth was the axis through the anterior and posterior midpoints of the spinal canal. Interfacial distance was the maximum distance between the two sides of the lateral border of the inferior articular process. The results are shown in Table 2.

Design of two thoracic fusion cages

In this study, two kinds of cages (box-shaped and kidney-shaped) made from a polyether ether ketone (PEEK) material were designed based on the anatomical parameters of the thoracic vertebras of the Chinese patients. The designs of the two cages fulfilled the following criteria:

1) Thoracic box–type interbody fusion cage–related anatomical parameters are as follows: maximum width (W1): as per the length of AB (Fig. 2) (distance between the tangent line of the lateral vertebrae and tangent line of the lateral spinal cord)/sin 45° = 0.5× (EW-spinal canal width) sin 45°; maximum length (L1): as shown in Fig. 2 height: as per the height of median disc height.
2) Thoracic kidney–type interbody fusion cage–related anatomical parameters are as follows: maximum width (W2) similar to W1; maximum length (L2): based on EW and height (H): the same as the box-typed cage.

The two thoracic cages, which could be easily and safely placed into the thoracic intervertebral space, were designed based on these anatomical results.

Finite element model of the thoracic spine (T10-T12)

The finite element model of the two thoracic intervertebral spaces (T10-T12) based on previous CT scans parameters was established, and the simulation of new cages used for TTIF was performed based on this model. Given that the T11-T12 intervertebral space requires more stability and suffers more stress, we chose levels T11-T12 as our FEA model.

The scans were saved in DICOM format and analysed using Mimics 17.0 and ANSYS 15.0 America, with the following steps. (1) Build the geometric model: the DICOM format T10-T12 segmental CT tomographic images were imported into Mimics 17.0 software. The 3D model of T10-T12 was established and remeshed, then the 3D model was output and saved in LIS format. (2) Build a finite element model: the geometric model was imported into the ANSYS 15.0 software to generate the three-dimensional finite element model of T10-T12. The generated model has 3055631 units and 1850437 nodes. (3) Material assignment. (4) Boundary conditions and loading model were established: the lower endplate of the T12 vertebral activity was limited, a vertical load of 400N on the upper surface of the T10 vertebral body, and 10 Nm of flexion, extension, left and right lateral flexion and axial torque were separately loaded on the T10 vertebral level (The vertical load of the T10 is

Table 2
Measurement of anatomical parameters of the endplate, spinal cord and facet joint in thoracic vertebrae (mm).

	Endplate			Spinal cord		Facet joint
	EW	MSDE	PSDE	SCW	SCD	IFD
T10/11	37.54 ± 3.36	28.86 ± 2.81	29.38 ± 3.05	17.77 ± 1.83	15.45 ± 1.36	34.41 ± 3.26
T11/12	40.18 ± 3.58	29.59 ± 2.86	30.51 ± 3.05	21.11 ± 2.11	17.02 ± 1.49	35.31 ± 2.90

EW, endplate width; MSDE, median sagittal diameter of endplate; PSDE, paramedian sagittal diameter of endplate; SCW, spinal canal width; SCD, spinal canal depth; IFD, interfacial distance.

measured in accordance with the influence of gravity of the model [14], and the load is less than the gravity of the whole body. The loading model of 10 Nm of flexion, extension, left and right lateral flexion, and axial torque were established based on the previous research about FEA model in lower thoracic vertebrae [15,16]). (5) Model confirmed: the average stiffness of the four models is compared with the previous literature [17] to confirm the validity of the three-dimensional finite element model. (6) Observation: displacement and mean stiffness values of the T10-T12 segments under different loading conditions were observed, shift and stress cloud maps were respectively established after identifying the stress distribution.

Statistical analysis

Statistical analysis was performed using SPSS 18.0 data analysis software (SPSS, USA). All values are expressed as mean ± SD. The difference among groups was detected using the one-way analysis of variance test. $P < 0.05$ was considered significantly different.

Results

Anatomical parameters and cages design

A total of 150 patients aged 18–81 years (average 53.8 ± 13.1 years) were reviewed. The anatomical parameters of the thoracic vertebra in the sagittal position, endplate, spinal cord, and facet joint in the thoracic vertebrae are listed in Tables 1 and 2.

Using Mimics software, two interbody cages (box-shaped and kidney-shaped) were designed as per their anatomical parameters (length, width and height) (Table 3). Moreover, the shape of these cages is shown in Fig. 3 (box-shaped cages and kidney-shaped cages in Fig. 3A and B, respectively).

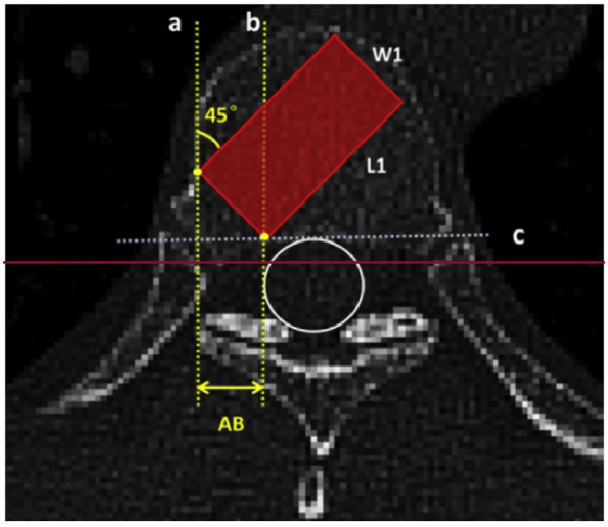

Figure 2. Measurement of box shaped cage: Inserted cage is at the 45° angle to the sagittal plane. Line a: tangent line of the lateral vertebrae. Line b: tangent line of the lateral spinal cord. Line c: tangent line of the dorsal vertebrae. W1: the maximum width of interbody fusion cage. L1: the maximum length of interbody fusion cage. AB: distance between the tangent line of the lateral vertebrae and tangent line of the lateral spinal cord.

Finite element model

Displacement model

Under the displacement working condition, the shift of T11-T12 segments [A (box-shaped cage), B (kidney-shaped cage), C (bone grafting model), and D (physical spine)] is shown in Fig. 4. The displacement cloud image showed that the movement of the T11-T12 segment in flexion, extension, lateral flexion and axial rotation were obviously restricted than the physical spinal cord, the shift of the surgical segments was reduced by approximately 87%–95%. The shift of surgical segments is frequently observed in model C but less frequently in model B. Thus, the kidney-shaped fusion cage had the best intervertebral stability.

Stress models

Under stress working conditions, the stress of the two kinds of cages [A (box-shaped cage), B (kidney-shaped cage)] is shown in Fig. 5. Stress cloud images revealed that the von Mises stress was evenly distributed in two cages, and there were no highly focused stress areas. However, the box-shaped cage had a larger stress peak than the kidney-shaped cage in all working conditions.

Discussion

TSS is common among the East Asian population, which can become a heavy burden to the family and society. Surgery is the best treatment option. Because of the support of ribs, thoracic vertebrae tend to be more stable than lumbar vertebrae. For the patients with TSS caused by dorsal compression, such as ossification of the ligamentum flavum, posterior decompression and internal fixation is needed. For posterior decompression may break the balance of the thoracic vertebrae, the surgical segment may not maintain physiological curve, even induce further thoracic kyphosis. However, TSS caused by dorsal compression do not need disc discectomy and cage implantation. Current indications for TTIF include, thoracic disc herniation (or combined with ossification of the posterior longitudinal ligament, ossification of the ligamentum flavum, thoracic fracture), ossification of the posterior longitudinal ligament (or combined with ossification of the ligamentum flavum), thoracic spine fracture or dislocation, thoracic spine tuberculosis and thoracic spine tumours. This study is based on TTIF, hence only TSS combined with ventral compression are relevant. TTIF is a good surgical process for thoracic compression. However, the lack of available anatomical parameters of Chinese patients and thoracic interfusion cages restricted its progress. Without an appropriate thoracic fusion cage, the compression bone grafting is commonly performed for interbody fusion. Patients who

Table 3
Parameters of the two newly designed fusion cages (mm).

	Width	Height	Length (L1/L2)	
	W	H	Box shape (L1)	Kidney shape (L2)
T10/11	15.28 ± 2.17	7.33 ± 0.84	28.58 ± 2.89	37.54 ± 3.36
T11/12	15.35 ± 2.25	7.85 ± 1.05	30.24 ± 3.09	40.18 ± 3.58

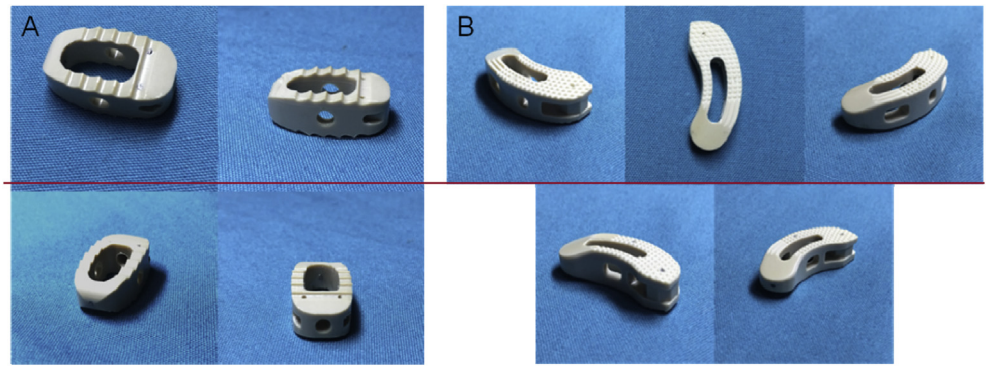

Figure 3. (A) The physical pictures of the box-shaped fusion cage. (B) The physical pictures of the kidney-shaped fusion cage.

had undergone compression bone grafting may have weaker biomechanical strength and insufficient support, which would increase stress in the fixation system and result in rod breaks, pedicle screw pull-out, and so on [7,9]. Interbody fusion cage could provide immediate segmental stability and good biomechanical environment, as well as minimise trauma in interbody fusion surgery [18,19].

To design a specific thoracic fusion cage, the thoracic anatomical parameters, cage biomaterials, and cage biomechanical stability should all be taken into consideration. In this study, the thoracic CT scans of 150 patients admitted to our institution were collected to obtain accurate thoracic anatomical parameters, and the cages were designed based on these anatomical parameters. PEEK material is close to the human bone

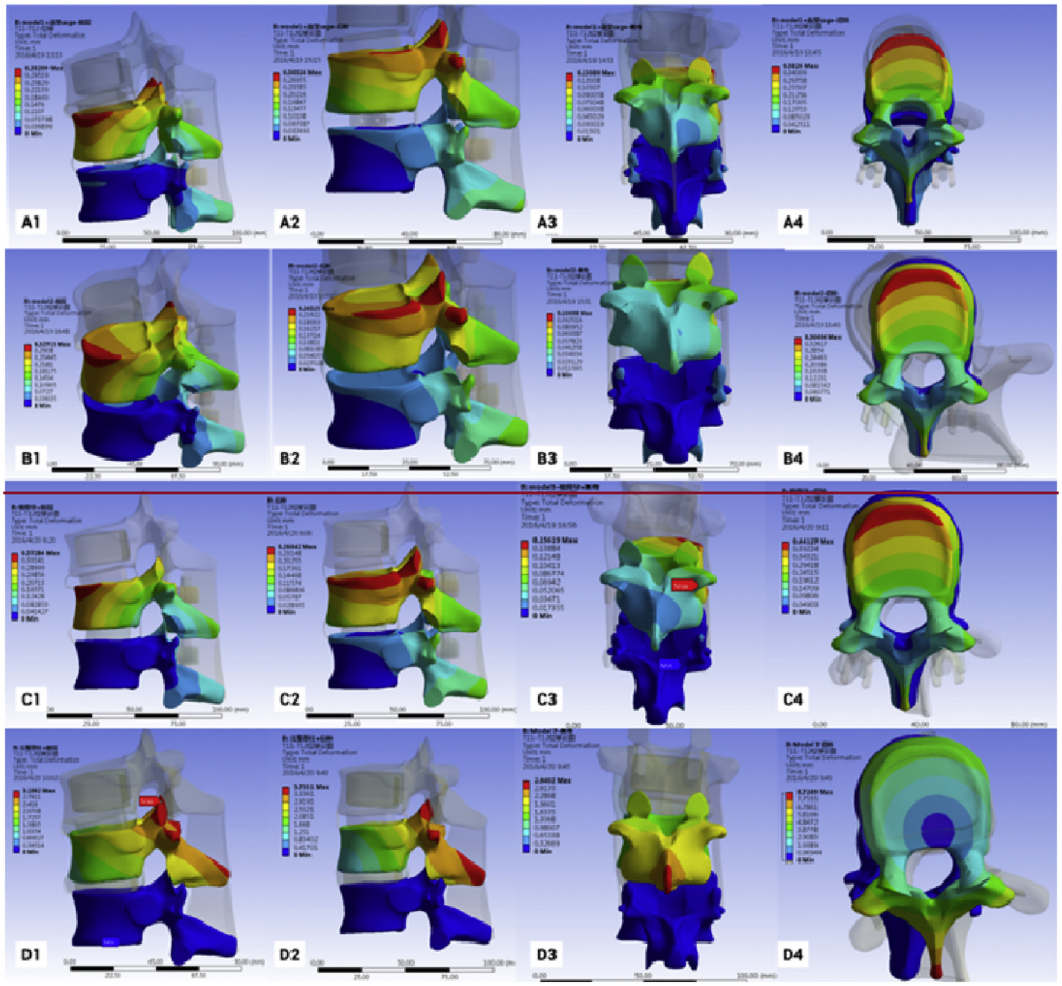

Figure 4. (A1-4): The box shaped cage movement cloud image of the T11-T12 segment. (A1):flexion working condition, (A2):extension working condition (A3) lateral flexion working condition (A4) axial rotation working condition. (B1-4): The kidney shaped cage movement cloud image of the T11-T12 segment. (B1):flexion working condition, (B2):extension working condition (B3) lateral flexion working condition (B4) axial rotation working condition. (C1-4): The bone grafting model movement cloud image of the T11-T12 segment. (C1):flexion working condition, (C2):extension working condition (C3) lateral flexion working condition (C4) axial rotation working condition. (D1-4): The physical spine movement cloud image of the T11-T12 segment. (D1):flexion working condition, (D2):extension working condition (D3) lateral flexion working condition (D4) axial rotation working condition.

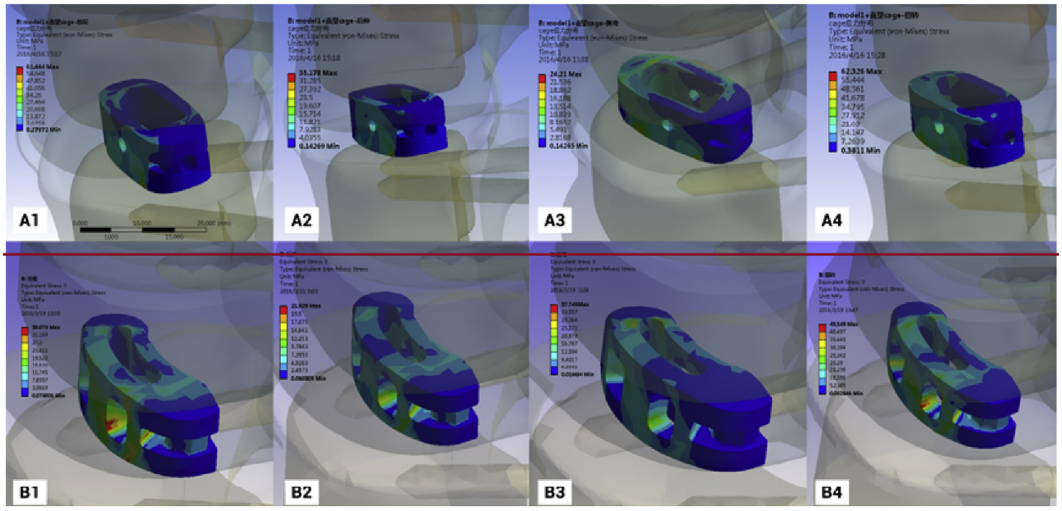

Figure 5. (A1-4):Box shaped cage stress cloud image of the T11-T12 segment. (A1) flexion working condition (A2) extension working condition (A3) lateral flexion working condition (A4) axial rotation working condition. (B1-4):Kidney shaped cage stress cloud image of the T11-T12 segment. (B1) flexion working condition (B2) extension working condition (B3) lateral flexion working condition (B4) axial rotation working condition.

tissue [20,21] and is superior to titanium in terms of the enhancement of intervertebral fusion [22,23], therefore, PEEK materials are an ideal material for thoracic fusion cages.

Compared with bilateral cage implantation, previous research has shown that unilateral cage implantation has the following advantages: less operative time, less bleeding, lower medical cost, and shorter hospital stay [21]. Moreover, in the biomechanical analysis, unilateral cage implantation had similar biomechanical stability and may result in increased interbody bone formation [24,25]. FEA has been widely used to evaluate biomechanical statistics and to make prognosis [26–28]. In this study, unilateral transplantation is applied and verified in our model; the fusion cage should be inserted through a 45° unilateral approach. The preclinical biomechanical assessments of the two kinds of thoracic cages were performed. The result showed kidney-shaped cage gained better stability than box-shaped cage, for the reason why could this occur need to be fully explored in our future experiment. At present, we suspect two potential events may influence their stability. First potential events may be that, the cage was implanted into intervertebrae through a unilateral approach, 45 degree from the central axis. After being inserted into the intervertebrae, the cage stays at a tilted positioin. Thus box-shaped cage could transmit excessive stress to the pedicle screw, suffering instability. Second, the contact area of the kidney-shaped cage is larger than the box-shaped one, and kidney-shaped cage contains longer curve, which fit intervertebrae, based on these events, kidney-shaped one may support better than box-shaped cage. All the two hypothesises need to be proved.

This study has several limitations. First, the FEA modelling process was simplified, which may not meet the physiological state of the spine. Second, the complex soft tissue environment around the spine, including paraspinal muscles, was neglected. Finally, more biomechanical properties of the two new cages, even TTIF and thoracic interbody fusion features, should be analysed.

In conclusion, our devices showed good biomechanical stability for interbody fusion. In addition, we demonstrated that the two interbody fusion devices were capable of accomplishing good stability in the intervertebral space. Notably, the kidney-shaped cage was better than the box-shaped cage.

Author contributions

Y.Y., W.L., and L.Y. contributed to research; H.Q. and T.N. analysed the data; Y.Z. conceived the study and participated in its design and coordination and drafting the manuscript; and all authors have read and approved the final manuscript.

Ethics approval

This study is approved by Ethics Committee of Peking Union Medical College Hospital, Beijing, China (permit number: S–K958).

Funding support

This work was supported by the National Natural Science Foundation of China, [Grant/Award Number: 81572093].

Conflict of interest

The authors have no conflicts of interest to disclose in relation to this article.

Acknowledgement

The authors would like to thank Dr. Yu Zhao, Ms. Wenjing Li, Mr. Lingjia Yu, Mr. Hao Qu and Mr. Tong Niu for their great support in this work.

References

[1] Ohtsuka K, Terayama K, Yanagihara M, Wada K, Kasuga K, Machida T, et al. A radiological population study on the ossification of the posterior longitudinal ligament in the spine. Arch Orthop Trauma Surg 1987;106:89–93.
[2] Machino M, Yukawa Y, Ito K, Nakashima H, Kato F. A new thoracic reconstruction technique "transforaminal thoracic interbody fusion": a preliminary report of clinical outcomes. Spine 2010;35:E1000–5.
[3] Ding WY, Guo Z, Zhang YZ, Shen Y, Li BJ, Zhang W, et al. Posterolateral transforaminal interbody fusion for thoracic disc herniation: a retrospective study of 38 cases. Orthop Surg 2009;1:280–4.
[4] Zhang HQ, Lin MZ, Shen KY, Ge L, Li JS, Tang MX, et al. Surgical management for multilevel noncontiguous thoracic spinal tuberculosis by single-stage posterior transforaminal thoracic debridement, limited decompression, interbody fusion, and posterior instrumentation (modified TTIF). Arch Orthop Trauma Surg 2012;132:751–7.
[5] Machino M, Yukawa Y, Ito K, Nakashima H, Kanbara S, Morita D, et al. Transforaminal thoracic interbody fusion" in the management of lower thoracic spine fracture dislocations: technical note. J Spinal Disord Tech 2013;26:E209–14.

[6] Kang CN, Cho JL, Suh SP, Choi YH, Kang JS, Kim YS. Anterior operation for unstable thoracolumbar and lumbar burst fractures: tricortical autogenous iliac bone versus titanium mesh cage. J Spinal Disord Tech 2013;26:E265–71.
[7] Cardenas RJ, Javalkar V, Patil S, Gonzalez-Cruz J, Ogden A, Mukherjee D, et al. Comparison of allograft bone and titanium cages for vertebral body replacement in the thoracolumbar spine: a biomechanical study. Neurosurgery 2010;66:314–8. discussion 8.
[8] Gao Y, Ou Y. Comparison between titanium mesh and autogenous iliac bone graft to restore vertebral height through posterior approach for the treatment of thoracic and lumbar spinal tuberculosis 2017;12:e0175567.
[9] Antoni M, Charles YP, Walter A, Schuller S, Steib JP. Fusion rates of different anterior grafts in thoracolumbar fractures. J Spinal Disord Tech 2015;28:E528–33.
[10] Berjano P, Blanco JF, Rendon D, Villafane JH, Pescador D, Atienza CM. Finite element analysis and cadaveric cinematic analysis of fixation options for anteriorly implanted trabecular metal interbody cages. Eur Spine J: Off Publ Eur Spine Soc, Eur Spinal Deform Soc, Eur Section Cervical Spine Res Soc 2015;24(Suppl 7): 918–23.
[11] Bashkuev M, Checa S, Postigo S, Duda G, Schmidt H. Computational analyses of different intervertebral cages for lumbar spinal fusion. J Biomech 2015;48: 3274–82.
[12] Schmidt H, Galbusera F, Rohlmann A, Shirazi-Adl A. What have we learned from finite element model studies of lumbar intervertebral discs in the past four decades? J Biomech 2013;46:2342–55.
[13] Yu L, Li B, Yu Y, Li W, Qiu G, Zhao Y. The relationship between dural ossification and spinal stenosis in thoracic ossification of the ligamentum flavum. J Bone Joint Surg Am Vol 2019;101:606–12.
[14] Xu G, Fu X, Du C, Ma J, Li Z, Tian P, et al. Biomechanical comparison of mono-segment transpedicular fixation with short-segment fixation for treatment of thoracolumbar fractures: a finite element analysis. Proc Inst Mech Eng H J Eng Med 2014;228:1005–13.
[15] Qiu TX, Teo EC, Lee KK, Ng HW, Yang K. Validation of T10-T11 finite element model and determination of instantaneous axes of rotations in three anatomical planes. Spine 2003;28:2694–9.
[16] Qiu TX, Teo EC, Zhang QH. Effect of bilateral facetectomy of thoracolumbar spine T11-L1 on spinal stability. Med Biol Eng Comput 2006;44:363–70.
[17] Wang ZL, Teo JC, Chui CK, Ong SH, Yan CH, Wang SC, et al. Computational biomechanical modelling of the lumbar spine using marching-cubes surface smoothened finite element voxel meshing. Comput Methods Progr Biomed 2005;80: 25–35.
[18] Li J, Dumonski ML, Liu Q, Lipman A, Hong J, Yang N, et al. A multicenter study to evaluate the safety and efficacy of a stand-alone anterior carbon I/F Cage for anterior lumbar interbody fusion: two-year results from a Food and Drug Administration investigational device exemption clinical trial. Spine 2010;35: E1564–70.
[19] Cho W, Wu C, Mehbod AA, Transfeldt EE. Comparison of cage designs for transforaminal lumbar interbody fusion: a biomechanical study. Clin Biomech 2008;23:979–85.
[20] Vadapalli S, Sairyo K, Goel VK, Robon M, Biyani A, Khandha A, et al. Biomechanical rationale for using polyetheretherketone (PEEK) spacers for lumbar interbody fusion-A finite element study. Spine 2006;31:E992–8.
[21] Kersten RF, van Gaalen SM, de Gast A, Oner FC. Polyetheretherketone (PEEK) cages in cervical applications: a systematic review. Spine J: Off J North Am Spine Soc 2015;15:1446–60.
[22] Chou YC, Chen DC, Hsieh WA, Chen WF, Yen PS, Harnod T, et al. Efficacy of anterior cervical fusion: comparison of titanium cages, polyetheretherketone (PEEK) cages and autogenous bone grafts. J Clin Neurosci: Off J Neurosurg Soc Australasia 2008;15:1240–5.
[23] Niu CC, Liao JC, Chen WJ, Chen LH. Outcomes of interbody fusion cages used in 1 and 2-levels anterior cervical discectomy and fusion: titanium cages versus polyetheretherketone (PEEK) cages. J Spinal Disord Tech 2010;23:310–6.
[24] Murakami H, Horton WC, Tomita K, Hutton WC. A two-cage reconstruction versus a single mega-cage reconstruction for lumbar interbody fusion: an experimental comparison. Eur Spine J: Off Publ Eur Spine Soc, Eur Spinal Deform Soc, Eur Section Cervical Spine Res Soc 2004;13:432–40.
[25] Chiang MF, Zhong ZC, Chen CS, Cheng CK, Shih SL. Biomechanical comparison of instrumented posterior lumbar interbody fusion with one or two cages by finite element analysis. Spine 2006;31:E682–9.
[26] Cahill PJ, Wang W, Asghar J, Booker R, Betz RR, Ramsey C, et al. The use of a transition rod may prevent proximal junctional kyphosis in the thoracic spine after scoliosis surgery: a finite element analysis. Spine 2012;37:E687–95.
[27] Clin J, Aubin CE, Parent S. Biomechanical simulation and analysis of scoliosis correction using a fusionless intravertebral epiphyseal device. Spine 2015;40: 369–76.
[28] Henao J, Labelle H, Arnoux PJ, Aubin CE. Biomechanical simulation of stresses and strains exerted on the spinal cord and nerves during scoliosis correction maneuvers. Spine Deform 2018;6:12–9.